SAND2023-13762J

A hybrid chemical-biological approach can upcycle mixed plastic waste with reduced cost and carbon footprint

Chang Dou[1,2], Hemant Choudhary[3,4,*], Zilong Wang[3,5,6], Nawa R. Baral[2,3], Mood Mohan[3,4], Rolin A. Aguilar[1,7], Shenyue Huang[1,5], Alexander Holiday[8], D. Rey Banatao[8], Seema Singh[3,4], Corinne D. Scown[2,3,9,10], Jay D. Keasling[2,3,5,11,12,13], Blake A. Simmons[2,3], Ning Sun[1,2,14,*]

[1] Advanced Biofuels and Bioproducts Process Demonstration Unit, Lawrence Berkeley National Laboratory, Emeryville, CA, 94608, USA

[2] Biological Systems and Engineering Division, Lawrence Berkeley National Laboratory, Berkeley, CA, 94720, USA

[3] Joint BioEnergy Institute, Emeryville, CA, 94608, USA

[4] Department of Bioresource and Environmental Security, Sandia National Laboratories, Livermore, CA, 94551, USA

[5] Department of Chemical & Biomolecular Engineering, University of California, Berkeley, CA, 94720, USA

[6] QB3 Institute, University of California, Berkeley, CA 94720, USA

[7] Department of Chemistry, University of California, Berkeley, CA, 94720, USA

[8] X, The Moonshot Factory, Mountain View, CA, 94043, USA

[9] Energy Analysis & Environmental Impacts Division, Lawrence Berkeley National Laboratory, Berkeley, CA, 94720, USA

[10] Department of Bioengineering, University of California, Berkeley, CA 94720, USA

[11] Energy & Biosciences Institute, Berkeley, CA, 94720, USA

[12] Center for Synthetic Biochemistry, Institute for Synthetic Biology, Shenzhen Institutes of Advanced Technologies, Shenzhen 518055, China

[13] Novo Nordisk Foundation Center for Biosustainability, Technical University of Denmark, Kongens Lyngby, Denmark.

[14] Lead Contact:

[*] Correspondence: hchoudh@sandia.gov (H.C.), nsun@lbl.gov (N.S.)

Summary

Derived from renewable feedstocks, such as biomass, polylactic acid (PLA) is considered a more environmentally-friendly plastic than conventional petroleum-based polyethylene terephthalate (PET). However, PLA must still be recycled and its growing popularity and mixture with PET plastics at the disposal stage poses a cross-contamination threat in existing recycling facilities and results in low-value and low-quality recycled products. Hybrid upcycling has been proposed as a promising sustainable solution for mixed plastic waste; but its techno-economic and lifecycle environmental performance remain understudied. Here we propose a hybrid upcycling approach using a biocompatible ionic liquid (IL) to first chemically depolymerize plastics, then convert the depolymerized stream via biological upgrading with no extra separation. We show that over 95% of mixed PET/PLA was depolymerized into their respective monomers, which then served as the sole carbon source for the growth of *Pseudomonas putida*, enabling the conversion of the depolymerized plastics into biodegradable polyhydroxyalkanoates (PHA). In comparison to conventional commercial PHA, the estimated optimal production cost and carbon footprint are reduced by 62% and 29%, respectively.

Keywords: polylactic acid (PLA), polyethylene terephthalate (PET), ionic liquid (IL), cholinium lysinate, depolymerization, waste recycling, *Pseudomonas Putida*, Polyhydroxyalkanoates (PHA), techno-economic analysis, life-cycle assessment

Introduction

Plastics are ubiquitous in modern life. Due to their superior functional properties and low cost, the application of plastics has been expanding in almost all aspects of our life. Global plastic production has continually increased over the past half-century, totaling 391 million metric tons in 2021.[1] Due to the limited end-of-life solutions, most of these plastics end up in landfills or are leaked into the environment, contributing to the accumulation of microplastics and threatening oceans and wildlife.[2,3] Beyond environmental implications, the current "take-make-waste" linear plastic system consumes fossil fuels and contributes to greenhouse gas (GHG) emissions.[4] A 2016 study found that nearly 6% of the world's oil production is used to produce plastics; that number is expected to expand to 20% by 2050, attributing to 15% of the global annual carbon budget - a significant level that should be taken seriously.[5] Cost-effective and energy-efficient processes for recycling or valorizing plastic waste streams are desperately needed to reduce the use of fossil fuel and divert plastic waste from landfills and the environment.[6]

A key challenge in recycling plastics is the commingling of different plastics in the recycling stream. Cross-contamination has significant ramifications including added burdens to the sorting process, decreased value of the recycled plastics, and compromised properties of recycled polymers. Polyethylene terephthalate (PET) is the most prevalent polyester and ranked as the most recycled plastic in the US.[7] Another polyester, polylactic acid (PLA) is a desirable plastic to consumers as it is bio-based and degradable, but still needs to be recycled. With the rapid expansion of the PLA market, there has been an increasing concern that more PLA will be present as contaminants that interfere to the existing PET recycling processes.[8,9] In particular, similar appearances, chemical functional groups, and applications of PET and PLA lead to new waste stream separation challenges in plastic recycling facilities including mechanical recycling of

PET.[8,10] While state-of-the-art sorting technologies (e.g. near infrared light) can distinguish between polymers such as PLA and PET, some cross-contamination remains unavoidable due to errors in mechanical sortation, especially given the vast volumes of waste processed in modern materials recovery facilities (MRFs).[9,11] Furthermore, the viability of incorporating a new plastic variant into MRFs is hindered by the expense linked to acquiring dedicated optical sorters and bunkers.[8,11] .

Chemical recycling has been highlighted as an alternative route to conventional mechanical recycling in dealing with cross-contaminated plastics.[6,12,13] The depolymerized products, usually monomeric precursors of plastics, can be separated and resynthesized into new polymers that maintain properties comparable to virgin plastics. Most chemical recycling of plastics involves catalysts such as metal-based catalysts and organocatalysts.[14–19] For instance, Pt, Sn, Ru, Ni, Ir, Al-based catalysts have been commonly employed in either plastic degradation or modification.[14–17] In a recent study, Sullivan et al. demonstrated a chemical process that employed Co(II) and Mn(II) co-catalysts in the autoxidation of mixed plastics.[19] After precipitation of Co/Mn catalysts as respective hydroxides, the oxidized stream was biologically valorized into bioproducts. However, metal-based catalysts can suffer from abundance scarcity or leaching of metallic sites into the solution increasing complexity in downstream processing including separation or microbial conversion.[19–21] Organocatalysts are considered as promising "green" substitutes to traditional metal-based catalysts.[18] Among the organocatalysts, ionic liquids (ILs, organic salts with melting point below 100 ºC) have proven to be catalytically efficient and are able to achieve high depolymerization and product yield for different types of plastics.[18] One of the most important characteristics of ILs is their tunable properties, a function of the specific combinations of cations and anions, making them task-specific.[22,23]

While many studies have utilized ILs to depolymerize PET and PLA, the majority of these depolymerization efforts were restricted to applying either pure ILs or ILs in organic solvents on individual polymers.[24–28] There has been relatively little emphasis on hydrolytic depolymerization of mixed plastics using ILs. Water is a good solvent for chemical reaction in terms of cost, process safety, and environmental impact. Applying water as the solvent also allows the potential biological use of depolymerized PET and PLA *via* microorganisms, as microbes have shown capabilities to consume terephthalate and lactic acid as the carbon sources.[29–34] A hybrid process that integrates bio-compatible chemical depolymerization and biological conversion without the need for initial chemical reagent separations would not only demonstrate an avenue to upcycle the mixed PET and PLA, but also validate the hybrid conversion approach as a solution for organic waste management on a broader scale. However, research on IL-based hybrid upcycling approach for mixed PLA and PET waste, as well as a comprehensive understanding of the techno-economic feasibility and lifecycle environmental performance, remains limited.

Here we bridge the knowledge gap by demonstrating the hybrid conversion process, where the biological conversion does not require separation of chemical reagents used in the chemical depolymerization step. Through investigating hydrolysis of PET and PLA using different ILs in water, we identified cholinium lysinate [Ch][Lys] with the highest depolymerization efficiency and monomeric product yields. This observation agreed with the results of molecular dynamic simulations, where [Ch][Lys] showed stronger polymer interaction over other studied ILs. Over 95% of theoretical monomer yields were achieved when applying [Ch][Lys] in hydrolytic depolymerization of PET and PLA mixture. *Pseudomonas putida* showed capability to utilize IL-depolymerized PET/PLA mixture as the carbon sources without additional feed of glucose. The use of aqueous biocompatible ILs eliminates the need for any separation steps before

bioconversion. Based on that, we conceptualized a one-pot process to upcycle mixed PET and PLA into polyhydroxyalkanoates (PHA) for techno-economic analysis (TEA) and life-cycle analysis (LCA). The optimal production cost and carbon footprint of PHA are estimated to reach \$0.95/kg and 1.7 kgCO_2e/kg, respectively, representing a reduction of 62% and 29% compared to commercially produced PHA. Overall, our findings suggest that the hybrid upcycling approach holds promise as an economically and environmentally sustainable solution for closing the life-cycle loop of cross-contaminated plastic wastes.

Results and Discussion

Screening of ILs in depolymerization of PET and PLA

ILs have been employed to depolymerize individual polyesters such as PET and PLA.[18,25] Most of them are conventional imidazolium-based, including the ones that contain halometallates. With the progress in the IL research, economic and biocompatible cholinium-based ILs have attracted high interest.[35,36] Building upon this, the current study explored two cholinium-based ILs, cholinium lysinate ([Ch][Lys]) and cholinium phosphate ($[Ch]_3[Phos]$), along with two imidazolium-based ILs, 1-ethyl-3-methylimidazolium acetate ($[C_2C_1im][Ac]$) and 1-ethyl-3-methylimidazolium chloride ($[C_2C_1im]Cl$). The reaction temperatures (180 °C for PET and 130 °C for PLA) were set below the melting point of the employed PET (235 °C) and PLA (153 °C), as the main purpose is to compare the catalytic efficiency of different ILs in polyester depolymerization. Continuous stirring was employed throughout the depolymerization reaction process (details in the experimental procedures). Figure S1A demonstrates the appearance before and after reaction.

Figure 1 shows the depolymerization efficiency and product yield of PET and PLA using different aqueous ILs. The depolymerization efficiency of PET and PLA ranged widely across different ILs. Both polymers shared the same trend in response to IL depolymerization with the cholinium-based ILs demonstrating higher catalytic activity compared to the imidazolium-based ILs after 2 h reaction. In particular, [Ch][Lys] had the highest depolymerization efficiency – 54.7% and 40.2% for PET and PLA, respectively. Terephthalic acid (TPA) and lactic acid (LA) were obtained as the degradation products of PET and PLA, respectively. Consistent with the depolymerization efficiency, the product yield followed the same trend in descending order of [Ch][Lys] > $[Ch]_3$[Phos] > $[C_2C_1im][Cl]$ > $[C_2C_1im][Ac]$. When using [Ch][Lys] as the catalyst, a maximum yield of 56.3% and 39.3% was achieved for TPA and LA, respectively. Conversely, depolymerization and product yield were negligible in the presence of $[C_2C_1im][Ac]$, indicating little IL catalytic activity under the given reaction condition. Note that both chloride and acetate salts of $[C_2C_1im]^+$-cation exhibited limited hydrolysis of both polyesters in contrast to previous report on hydrolysis of PLA using 1-butyl-3-methylimidazolium ($[C_4C_1im]^+$) ILs, where $[C_4C_1im][Ac]$ outperformed all other anion combination.[28] The difference in activity is supposedly due to the shorter side-chain of IL cation and higher amount of water in the present study. It should be noted that water, even in small amounts, has been known to influence IL physicochemical properties under certain operating conditions,[37] and this could explain the differences between the two studies.

Hydrolytic depolymerization of PET and PLA involves chain scission of ester linkages, where a carboxyl end group is released. PET and PLA depolymerization can occur under base catalysis, as the hydroxide ion deprotonates the oxygen atom of water and increases its nucleophilicity in attacking the ester groups. The pH of the reaction solution before and after depolymerization

reaction (Table S1) aligns with the depolymerization efficiency across ILs, where cholinium-based ILs demonstrated higher pH over imidazolium-based ILs. To evaluate whether the pH influenced by IL was the major driving force of PET and PLA depolymerization, a set of control experiments were conducted using only water and alkaline water as the solvent (Figure 1). For the alkaline water, 0.006 M of NaOH was added to adjust the pH to mimic that of employed aqueous [Ch][Lys] (with pH 11.8). Surprisingly, the pH adjusted reaction system showed no difference versus the water control; both PET and PLA were barely depolymerized with negligible product yields. Our findings were different from some previous studies where alkaline conditions formed by 0.6-1.3 M NaOH (pH ≥ 13) were found to facilitate the depolymerization of PET and PLA.[38,39] This is likely due to the relatively lower NaOH molarity (and lower pH) in our control, as the PET hydrolysis has been shown to be positively correlated with NaOH concentration.[40] These control experiments, along with literature reports, strongly indicate that PET and PLA hydrolysis under the applied conditions require either higher concentrations of hydroxyl ions or possible intermolecular interactions with IL to enhance the hydrolytic cleavage. Understanding the intermolecular interactions between IL and polymer would be thus necessary.

Water-soluble fractions were analyzed to understand the depolymerization of plastics under the tested conditions. Molecular weight distribution profiles of the depolymerized stream from each polymer corroborate the observed product yield (Figure S2). Based on the calibration standards, [Ch][Lys]-based reaction solutions had signals on the far right (indicating the smallest MW fraction) while all other IL-based reaction mixtures showed presence of intermediate MW (less than 1500 Da) (Figures S2A-S2B). Interestingly, large MW fractions were obtained with alkaline water (that is in presence of NaOH) only but did not afford any notable signals corresponding to mono-, di-, or oligomers (Figures S2B-S2C). It should be stressed that PET glycolysis dominates

the literature compared to hydrolysis - where the GPC of the reaction mixture was not discussed in literature.

Molecular dynamics simulated polyester-IL interactions

To understand the effect of IL/water mixtures and water on the depolymerization of polyesters, molecular dynamics (MD) simulations were performed using PLA as a model substrate (Figure S3). MD simulations are a widely used computational method for examining the interactions between molecules in binary solutions and were employed in this study to explore the depolymerization mechanism of polyesters (Table S2).

To obtain the structural arrangements and microscopic interactions, radial distribution functions (*g(r)* or RDFs) between PLA and the investigated solvent systems were calculated. The RDF (*g(r)*) is defined as the probability of identifying a molecule at a distance of 'r' from the reference molecule.[41] The RDF plots are a powerful tool for analyzing the structural and explicit interactions between solute and solvent(s). In general, *g(r)* intensity is related to the strength of contact probability between the solute and solvent. In this study, the RDF was plotted between the oxygen (O) atom of the PLA molecule and the anion/cation of IL and water, and the results are depicted in Figure 2A-B. The first and largest solvation shell in Figure 2A exhibited at a distance of 2.65 Å between the PLA and cation of $[Ch]_3[Phos]$ and [Ch][Lys] with a *g(r)* intensity of 5 and 10, respectively, indicating that cholinium cation forms regular and definite coordination spheres around PLA at a distance of 2.65 Å, and the RDF plot was primarily dominated by the first coordination shell. While, for $[C_2C_1im][Ac]$/water, $[C_2C_1im]Cl$/water, and water systems, the RDF peak was attained at a distance of 2.2-2.35 Å with low *g(r)* value~1. These results agree with the

experimental results, that is, [Ch][Lys] has about two and ten times stronger contact probability with PLA compared to $[Ch]_3[Phos]$ and imidazolium-based IL systems, respectively. On the other hand, the RDF peak between PLA and anions of ILs obtained at a relatively higher distance with a lower *g(r)* value (Figure 2B), implying that cation may have a stronger contact probability with PLA than the anions in ILs. Further, the MD simulated non-bonded interaction energies (i.e., electrostatic and van der Waal (vdW) interactions) for PLA-IL systems were also computed and supported depolymerization efficiency using [Ch][Lys] (Figure S4). It is important to highlight that the stronger interactions between PLA-cation and PLA-anion were established in [Ch][Lys], thus the enhanced solvation of PLA with both $[Ch]^+$ and $[Lys]^-$ ions compared to other cation and anions in this study (Figure S4).

Furthermore, the RDF and number of hydrogen bonds (HBs) between water and anion of ILs have been calculated, and the results are shown in Figure 2C-D. The RDF peaks between the anions of IL and water were obtained at a distance of 2.65-2.85 Å with a *g(r)* intensity of ~2 to 5. Lysinate anion had shown lowest *g(r)* peak intensity, implying that the hydration (thereby the interaction with water) of lysinate anion was weaker compared to phosphate, acetate, and chloride anions (Figure 2C). This is further evidenced by computing the number of HBs between water and anions of IL (Figure 2D). From Figure 2D, the number of HBs between lysinate and water was relatively lower than other anions, validating the weaker hydration of $[Lys]^-$ anion. In other words, anions other than lysinate (i.e. phosphate, acetate, and chloride) are heavily surrounded by water molecules, leading to weaker contact probability with PLA and hence lower depolymerization efficiency.

In addition to MD simulations, Hansen solubility parameter (HSP) was also taken into consideration to understand why [Ch][Lys] outperformed other ILs studied here. HSP is a critical

property of a molecular species that analyzes polarity and quantifies the "like seeks like" principle. For instance, a given solute (e.g., PET or PLA) is considered to be highly miscible/soluble in a given solvent (ILs in the present case), if the HSP values of the solute and the solvent are similar. The HSP values of PET, PLA, ILs, and water are presented in Table S3. The total HSPs (δ_t) of PET and PLA are 21.66 $MPa^{1/2}$ and 20.87 $MPa^{1/2}$, respectively. On the other hand, the solubility parameter of [Ch][Lys] and $[Ch]_3[Phos]$ are 26.30 $MPa^{1/2}$, and 28.25 $MPa^{1/2}$ which are close to the PET and PLA's HSP values, suggesting higher miscibility of these polyesters in [Ch][Lys] and $[Ch]_3[Phos]$. In contrast, the solubility parameters of $[C_2C_1im][Ac]$, $[C_2C_1im]Cl$, and water are much higher than PET and PLA, implying that $[C_2C_1im][Ac]$, $[C_2C_1im]Cl$, and water have weaker affinity for these polyesters resulting in a lower depolymerization and conversion rates. Accordingly, it can be established that polyester depolymerization is largely influenced and governed by the choice of ion combination in any given IL. The order of solvent HSP values that is close to polyesters is as follows: [Ch][Lys] > $[Ch]_3[Phos]$ > $[C_2C_1im]Cl$ > $[C_2C_1im][Ac]$ > water, which is in line with the experimental observations.

Depolymerization of PET/PLA mixtures using [Ch][Lys]

As discussed previously, the current waste management facilities will not completely eliminate the PLA contamination when sorting PET for recycling. With the increasing prevalence of PLA, it is likely that more PLA will end up in the PET recycling stream. Herein, we prepared a PET/PLA mixture by combining PET and PLA at 1:1 mass ratio and investigated the IL-catalyzed hydrolysis of these polyester mixtures. Given its high catalytic activity, [Ch][Lys] was selected as the IL in the reaction. It should be emphasized that [Ch][Lys] is a favorable choice not only because of its

high depolymerization efficiency but also because it is economic, biocompatible, less toxic, and environmentally friendly.[35,42,43]

A range of IL loading (10-90 wt% [Ch][Lys]) was applied to maximize depolymerization efficiency and product yields of the PET/PLA mixture. The initial set of experiments was carried out at 160 °C for two hours. As Figure 3A shows, the depolymerization efficiency varied across different IL loadings. The depolymerization efficiency started low (50.8%) at 10 wt% IL loading and increased with the increasing IL loading, reaching up to 99.5% at 60 wt% IL loading. The product yields of TPA and LA followed a similar trend to depolymerization and peaked at 45 wt% IL loading, where the TPA and LA yields reached 79.6% and 93.8%, respectively. Interestingly, increasing the IL loading beyond 45 wt% did not show a benefit. While the depolymerization remained high at 60 wt% IL loading, the product yields were lower than that of 45 wt% IL loading (77.2% for TPA and 53.1% for LA). More surprisingly, at 90 wt% IL loading, that is pure IL (and no water), the depolymerization efficiency decreased to 91.5%. Meanwhile, the TPA yield turned to be negligible (1.5%) and the LA yield was merely 40.9%. The reasons are manifold. On one hand, the major hydrolytic reaction was found to occur on the external surface of polyester where the solubility is the reaction rate determining step.[27,40] ILs could dissolve PET and PLA to facilitate depolymerization at higher IL loading.[36,44,45] On the other hand, the lack of water likely impeded hydrolytic reaction and resulted in incomplete depolymerization. Both the product yields and the gel permeation chromatography (GPC) results provide clues to this explanation. At higher IL loadings of 60 and 90 wt%, GPC revealed partial depolymerization into monomers and oligomers along with partial (low molecular weight) polymer dissolution (Figure S2D). In this scenario, [Ch][Lys] was efficient in dissolving these polyesters at 160 °C (Figure S1B); whereas, in the absence of water, only a partial polyester depolymerization (i.e. hydrolysis) could be afforded.

Based on the yields of LA and TPA along with the molecular weight distribution profiles, the preferential depolymerization of PLA over PET is expected at higher IL loadings with limited/negligible water content.

Although [Ch][Lys] is considered as cost-competitive compared to other conventional ILs, IL usage is often the major cost contributor in the process economics.[46,47] In order to explore the way to reduce IL loading, a set of experiments was conducted by increasing the reaction time from 2 h to 6 h. Overall, the extension of reaction time improved both depolymerization and product yields at low IL loadings (Figure 3B). In particular, 20 wt% IL loading resulted in a high depolymerization (95.1%) with high product yields (TPA for 96.5% and LA for 96.6%). Additional reaction time did not benefit the product yields at 90 wt% IL loading. Despite increasing depolymerization from 91.5 to 97.1%, the TPA yield remained negligible (1.6%) and the LA yield decreased by half – possibly due to the degradation of the desired product.[10]

Overall, the yield of LA was higher than that of TPA. It is apparent that PLA is the major contributor to the depolymerization of PET/PLA mixture at 10 wt% and 20 wt% IL loadings. This is likely due to the fact that the PLA has lower glass transition (~62 °C) and melting point (153 °C) compared to PET (onset from 235 °C) (Figure S5). At 160 °C, the molten condition ensures a complete PLA mobility and facilitates the hydrolysis reaction,[28] whereas solubility remains the obstacle in PET hydrolysis.[27] Post-consumer PET and PLA were collected and tested under the conditions optimized for virgin polymer resins presented in Figure 3B. Under reaction conditions of 20 wt% [Ch][Lys] loading at 160 °C for 6 h, the post-consumer PET/PLA mixture (PET:PLA at 1:1 w/w ratio with 10 wt% polymer solid loading) achieved an 85.1% depolymerization efficiency, resulting in a 52.5% TPA yield and a 97.4% LA yield (Figure S6B). It should be noted that the calculation considered these substrates consist of 100% PET or PLA individually.

Compared to the virgin resins, the relatively lower depolymerization and monomer yield of post-consumer PET/PLA mixture can be explained by the difference between the starting substrates. It is known that plastic-based commodity products commonly contain impurities such as fillers and paints, among others, which decrease the polymer content (wt%) in these products.

Though not implemented in the current study, we anticipate the process of product recovery to be relatively simple. Because of the presence of [Ch][Lys], the pH of the reaction system is high (Table S1). TPA is water soluble under alkaline conditions, but is insoluble in acidic pH.[48] One can take advantage of this property and recover TPA by lowering the pH of the solution to precipitate out TPA. LA can be recovered as suggested in a previous study through the precipitation of lactate in the form of calcium lactate by adding calcium carbonate.[28] After filtration, the calcium lactate can then be converted back to water soluble lactic acid by adding a stronger acid. The IL remains in the solution and can be recycled and reused after necessary conditioning such as pH adjustment, salt removal, etc. It is important to highlight that these separation techniques add on economic and environmental burden, and thereby integrating bioconversion without additional separation could alleviate such burdens while opening avenues for existing and novel bioproducts.

One-pot bioconversion of depolymerized PET/PLA

In addition to separating and purifying the products for chemical applications, hydrolysis of PET and PLA provides a large amount of organic acids that can potentially serve as the carbon source pool for microbes. Herein, *Pseudomonas putida* was selected to investigate the microbial cell growth using the depolymerized PET/PLA mixture.[49,50] Two strains were used, including *P. putida*

KT2440 and *P. putida* TDM461; the former one is a widely used wide-type *P. putida* with potential for biomass conversion and the latter one is an engineered *P. putida* KT2440 strain with inserted TPA catabolic and transporter genes (*P. putida* Δ*hsdMR::*P_{tac}*:tphA2*$_{II}$*A3*$_{II}$*B*$_{II}$*A1*$_{II\text{-}E6}$ *fpvA:*P_{tac}*:tpaK*$_{RHA1}$).[51] Our previous studies have demonstrated successful fermentation processes using pretreated lignocellulosic biomass in the presence of [Ch][Lys].[43,46,47,52] In this study, supernatant of most efficiently depolymerized PET/PLA mixture (20 wt% [Ch][Lys] at 160 ℃ for 6 h) was subjected to different dilutions before feeding to *P. putida* KT2440 and *P. putida* TDM461 (Table S4). Overall, microbial cell growth was observed in dilutions ranging from 10 to 20-fold, indicating a sound fermentability of IL-depolymerized plastic mixture (Figure S7A-B).

For both strains, the highest cell density was obtained using media prepared with 20-fold dilution, which contains 1.6 g/L TPA and 3.1 g/L LA (Figure S6A). Not surprisingly, the cell growth of *P. putida* TDM461 was better than *P. putida* KT2440 in all scenarios. This is because *P. putida* TDM461 was engineered to consume TPA as an additional carbon source, whereas the KT2440 has not been reported with any TPA catabolic pathway. The cell growth in the media prepared with 10-fold dilution showed decreased cell density, with *P. putida* TDM461 sustained for a longer time. This is attributed to the higher toxicity from the increased [Ch][Lys] concentration (2.0 wt% IL for 10-fold dilution), which was evidenced when cells were grown with only IL (Figure S8A).

As the depolymerized PET/PLA contains multiple carbon sources (e.g. TPA, LA, and [Ch][Lys]), elucidation of the cell growth contributed from different carbon sources can be helpful for the fermentation with the depolymerized PET/PLA mixture. Accordingly, PET and PLA were depolymerized separately under 10 wt% polymer solid loading with 20 wt% [Ch][Lys] at 160 ℃ for 6 h, to evaluate the cell growth with the single carbon source. The corresponding depolymerized products were then diluted at gradients to formulate the media for cell growth tests

(Table S4). Figure 4 shows *P. putida* TDM461 cell growth with different media aforementioned. Overall, media formulated with the depolymerized PLA showed a more robust cell growth with shorter lag phases, higher cell densities, and a more stable stationary phase compared with the media formulated with the depolymerized PET. This result indicates that although *P. putida* TDM461 has been engineered to catabolize TPA, it still maintains the great ability to utilize LA. Notably, the presence of LA in the media formulated with the depolymerized PET/PLA enhanced the cell growth, showing higher cell densities and more stable stationary phase than using depolymerized PET alone. The results aligned well with the cell growth using culture media prepared with synthetic TPA and LA (Figure S8B-D). These findings demonstrate the potential of using depolymerized PET/PLA as direct carbon sources for microbial fermentation. Furthermore, the cell growth observed in the IL control confirmed that [Ch][Lys] also contributed to the growth of *P. putida* TDM461 (Figure 4 and Figure S8A). This is consistent with other studies that have found the cholinium catabolism of *Pseudomonas* species,[53–55] supporting the biocompatibility of [Ch][Lys] and its potential use in a one-pot process for the upcycling of mixed PET and PLA. It is worth noting that a gene knockout of cholinium catabolic pathway has been demonstrated to prevent the microbe from consuming the IL, thereby reducing the IL loss.[53]

One of the well-known fermentation products from *P. putida* is polyhydroxyalkanoates (PHA)，

a group of natural biodegradable polymers which offer a broad spectrum of applications.[56] *P. putida* strains, either wild type or engineered, have been reported to produce PHA from a wide range of carbon sources, including TPA derived from PET.[33,56,57] We believe that *P. putida* strains could be engineered to successfully ferment with the depolymerized PET/PLA mixture for PHA production. Based on this hypothesis, PHA production cost and carbon footprint were analyzed in the following section.

Economics and environmental impact of hybrid upcycling

The use of an aqueous solution of biobased and biocompatible IL (e.g. [Ch][Lys]) allows the direct utilization of depolymerized stream in biological conversion without extra separation steps. In this regard, we conceptualized a one-pot conversion technology that integrates chemical and biological conversion to upcycle polyester plastic mixture into valuable products (PHA in this case). To understand the process economics and environmental impact of this new technology, techno-economic assessment and life-cycle analysis were performed to evaluate the major cost and sustainability drivers in the one-pot plastic upcycling process.

The process model includes all the required PLA/PET mixture to PHA conversion processes, including plastics waste preprocessing, one-pot PLA/PET conversion to PHA, PHA recovery, wastewater treatment, onsite energy, and utility stages. The modeled upcycling facility for PET and PLA is assumed to be co-located with a waste sorting facility, which eliminates the costs and GHG emissions associated with transporting the sorted and baled material from the sorting facility to the conversion facility. Our analysis determines the production cost and carbon footprint of PHA based on the PET/PLA depolymerization results demonstrated in this study and the best-reported TPA/LA to PHA yield from prior studies, which is an average of 11.8 wt%.[33,58–60] In addition, we present the optimal production cost and carbon footprint of PHA assuming that the conversion rates reach near the theoretical limits, as shown in Table 1.

Figure 5 depicts the production cost and carbon footprint of biologically produced PHA by utilizing a mixture of PET and PLA. As expected, a low bioconversion yield at present (Table 1)

results in a relatively high production cost (Figure 5A) and carbon footprint (Figure 5D). The difference in the current and potential optimal PHA yields highlights a great opportunity to improve the biological conversions of PET and PLA derived products. Achieving a PHA yield of 50 g per 100 g of PET/PLA mixture while holding all other process parameters at their currently-demonstrated values significantly reduces the production cost (Figure 5C) and carbon footprint (Figure 5F). Even a PHA yield at ~30 g per 100 g of PET/PLA mixture observes a considerable cut on the production cost and carbon footprint by 45 and 39%, respectively (Figure 5C and 5F).

As Figure 5A and 5D shows, one-pot depolymerization and bioconversion accounts for 35% of the PHA production cost and 61% of its life-cycle GHG emissions. IL and process electricity contribute to 81% of the one-pot conversion stage cost and 96% of its GHG emissions, where electricity has a larger impact on the GHG emissions (33%) relative to the production cost (14%). The impact of IL cost can be reduced by decreasing makeup IL either by reducing its loading rate, increasing its recovery rate, or both. The impacts of electricity can be reduced by increasing solid loading for the depolymerization process. Increasing solid loading will reduce the volume of solvent (water and IL) entering the one-pot reactor that will reduce either size or number of reactors, thereby reducing the electricity consumption. This will also reduce capital cost not only for the one-pot depolymerization and bioconversion process but also for the downstream recovery, wastewater treatment, and onsite energy generation stages. These improvements are considered in the optimal future case scenario (Table 1). Notably, the carbon footprint of the U.S. electricity mix has been declining over the years due to increasing share of renewable electricity; electricity could be less influential to the carbon footprint of PHA in the future.

Onsite energy generation is another capital- and carbon-intensive process accounting for 31% of the PHA production cost and 11% of its GHG emissions (Figure 5A and 5D). This is mainly due

to the natural gas-based steam generation system considered in this analysis. Switching to a renewable steam generating system, such as geothermal or solar, and/or reducing the operating temperature of the depolymerization process can reduce the costs and carbon footprint contributions from the onsite energy generation stage. Lowering the operating temperature of the depolymerization process reduces cooling/chilled water demand for the one-pot process, which means it requires less energy for the utilities. The PHA extraction and recovery stage is also a capital-intensive process (21% of the total production cost) as it includes both PHA recovery and [Ch][Lys] recovery, which requires multiple separation and filtration units. Developing a consolidated PHA and IL recovery system could reduce the costs and carbon footprint impacts of the recovery stage. In addition, wastewater treatment accounts for 8% of the total PHA production cost and 19% of its carbon footprint at the current state of technology. Increasing the solid loading during PLA and PET depolymerization reduces the volume of water entering the one-pot process and could save the cost and energy consumption of water recovery in the wastewater treatment stage.

Achieving 90% of bioconversion yield of PHA and marginal improvements in other process parameters, including solid loading, IL loading and recovery rates, and solvent loading for PHA extraction (Table 1 and Table S5), the production cost and carbon footprint of PHA could reach \$0.95/kg (Figure 5B) and 1.7 $kgCO_{2e}$/kg (Figure 5D), respectively. These numbers are lower than the current market price (\$2.5/kg) and GHG emissions (2.4 $kgCO_{2e}$/kg) of sugar-derived PHA (Figure 5).[61,62] These optimal results are even lower than petroleum-derived PET selling price (~\$1/kg) and carbon footprint (2.7 $kgCO_{2e}$/kg).[63,64] Our study indicates that PET and PLA derived PHA provides a renewable plastic upcycling avenue that has the potential to enable affordable recycling and conversion of petroleum-based PET and biobased PLA mixtures into biodegradable

PHA. To eventually achieve commercial competitiveness at scale, however, a dramatic improvement in key cost and carbon footprint drivers, including TPA, LA, and EG to PHA conversions is required. Future studies could prioritize improving PET/PLA depolymerization rate at a lower ionic liquid loading rate (Figure S9). Improving production rate of PHA by reducing bioconversion time and designing an energy efficient one-pot reactor are also important before commercial deployment of the technology evaluated in this study. The reaction achieved over 95% theoretical yields of both TPA and LA with 20 wt% [Ch][Lys] loading at a reaction temperature of 160 °C for 6 h.

Conclusions

Cholinium- and imidazolium-based ILs were investigated to depolymerize PET and PLA in water, with TPA and LA as the target products. Among the investigated ILs, [Ch][Lys] showed better performance and was further studied in the depolymerization of PET/PLA mixture. The reaction achieved over 95% theoretical yields of both TPA and LA with 20 wt% [Ch][Lys] loading at a reaction temperature of 160 °C for 6 h. Given the biocompatibility of the IL, the depolymerized plastics were directly subjected to the biological conversion. An engineered *P. putida* showed robust growth when using media formulated with the depolymerized PET/PLA, though the cells still grew better using depolymerized PLA than using depolymerized PET alone. The findings reveal the potential of an IL-based one-pot conversion technology which integrates polymer hydrolysis and biological valorization of the plastics and plastic mixture. Waste plastics could serve as low or negative cost feedstock to provide a rich carbon source for microbial fermentation to produce advanced biofuels and bioproducts. Techno-economic analysis and life-cycle assessment results indicate that the process of a one-pot depolymerization and bioconversion of PET/PLA mixture into PHA could be cost competitive and achieve a low carbon footprint. The

process provides an innovative plastic upcycling avenue - converting both petroleum-based and bio-based plastics into biodegradable PHA. Further investigation is required to understand the technological impact and challenges posed by additional contaminants present in the PET/PLA wastes streams from various commodity products, especially those from materials recovery facility (MRF) on this approach. Future improvements, particularly enhancing biological conversion efficiency, are required to boost the economic viability of the process demonstrated in this work.

Experimental procedures

Resource availability

Lead contact

Further information related to the data and code described in the ‘‘experimental procedures’’ section should be directed to the lead contact, Ning Sun (nsun@lbl.gov).

Materials availability

Materials generated in this study will be made available on request, but we may require a payment and/or a completed materials transfer agreement if there is potential for commercial application.

Data and code availability

All data for the figures in the main text is available in the Zenodo repository: https://doi.org/10.5281/zenodo.7536211. Data or code for the figures in the supplemental information are available from lead contact upon request.

Materials

Both polyethylene terephthalate (PET) and polylactic acid (PLA) were obtained from Goodfellow. PET (Cat. ES306030) was received as powder with particle size of 300 micron. PLA (Cat. ME346310) was received as nominal granule (3-5mm) and further comminuted using a Wiley Mill (Thomas Scientific, Swedesboro, NJ) with a 2mm sieve. Differential scanning calorimetry (DSC, Mettler Toledo, Columbus, OH) analysis was performed to determine the glass transition temperature of the polymers, where the specific sample was heated from 25 to 325 °C at 10 °C/min heating rate with only one heating cycle. Figure S5 shows the melting temperature of PET and PLA is 153 °C and 235 °C, respectively. Post-consumer PET was prepared using the bottle of Kirkland Signature bottled water (Costco Wholesale Corporation, Issaquah, WA, USA). Post-consumer PLA was prepared using clear cold cups (NatureWorks, Minneapolis, MN, USA). Both post-consumer PET and PLA were cut into 1.0 x 1.0 cm flakes before the experiment (Figure S6).

Cholinium lysinate ([Ch][Lys]) was purchased from Proionic GmbH (Grambach, Austria), 1-ethyl-3-methylimidazolium chloride ($[C_2C_1im]Cl$) was purchased from Sigma–Aldrich (St. Louis, MO), and 1-ethyl-3-methylimidazolium acetate ($[C_2C_1im][Ac]$) was procured from BASF (Ludwigshafen, Germany). $[Ch]_3[Phos]$ was synthesized in-house according to the following procedure. In an oven-dried round-bottomed flask (RBF) containing a Teflon coated magnetic stirring bar, 0.15 mol of cholinium hydroxide (46 wt% aqueous solution) was weighed. The flask was mounted on an ice-bath and an additional funnel was attached to the RBF. An aqueous solution of 0.05 mol phosphoric acid was transferred to the addition funnel and added dropwise to the stirring cold solution of cholinium hydroxide. The mixture was then stirred for an additional 1 h after complete addition of the acid. Water was removed by freeze-drying the reaction mixture to obtain the dry $[Ch]_3[Phos]$.

Water was deionized, with a specific resistivity of 18 MΩ cm at 25°C, from Purelab Flex (ELGA, Woodridge, IL). A solution of 0.006 M NaOH was prepared and used as alkaline water control at pH of 11.8. All the other chemicals were purchased from Sigma–Aldrich (St. Louis, MO).

Depolymerization reaction and yield calculations

The depolymerization reaction of polyesters were conducted in a 15 mL pressure tube (Ace Glass Inc., Vineland, NJ). For reactions with individual plastic, 4.5 g of solvent (4.0 g of water + 0.5 g of IL) was added to 0.5 g of PET (or PLA) in a glass pressure tube containing a magnetic stir bar. The pressure tube was placed in a preheated oil bath, and the mixture was stirred at 400 rpm for 2 h at the target temperatures. The reaction temperatures were set at 180 °C for PET and at 130 °C for PLA. For reactions with PET/PLA mixture, 10 wt% polymer (PET:PLA 1:1, w/w), *x* wt% [Ch][Lys], and (90-*x*) wt% water were mixed and reacted at 160 °C for either 2 h or 6 h.. The tube was immersed in a preheated oil bath at a desired temperature. Upon completion of the reaction, the tube was taken out from the oil bath and cooled to room temperature.

The reaction residue was transferred to a 50 mL falcon tube, where solid residue was recovered through centrifugation. The solid fraction was washed with deionized water three times before being dried in a lyophilizer (Labconco, Kansas City, MO). The liquid fraction was sampled for product analysis. The depolymerization and product yield are defined in eq.(1) and eq.(2), respectively:

$$Depolymerization = \frac{W_{substrate} - W_1}{W_{substrate}} \times 100\% \quad (1)$$

$$Yield = \frac{W_{product}/M_{product}}{W_{substrate}/M_{substrate}} \times 100\% \quad (2)$$

where $W_{substrate}$, W_1, and $W_{product}$ corresponds to the weight of starting polymer substrate, the weight of residual polymer, and the weight of monomeric products after depolymerization (TPA from

PET and LA from PLA), respectively. $M_{product}$ represents the molecular weight of TPA or LA; and $M_{substrate}$ represents the molecular weight of repeating units in each polyester.

Product analysis

Terephthalic acid (TPA) and lactic acid (LA) were measured on a Thermo Scientific Ultimate 3000 HPLC (Waltham, MA, USA) equipped with a Bio-Rad Aminex HPX-87H column (300x7.8 mm, Hercules, CA, USA). 4 mM sulfuric acid was used as the mobile phase at a flow rate of 1.0 mL/min. The column oven temperature was maintained at 65 °C. TPA was quantified by an ultraviolet (UV) detector at 240 nM, LA was quantified by a refractive index (RI) detector held at 55 °C.

Molecular weight distribution analysis

Molecular weight distribution of the reaction mixtures was measured through gel permeation chromatography (GPC). The analysis was performed on an Agilent 1260 infinity LC instrument equipped with a refractive index detector and a PL aquagel-OH column (Agilent, Santa Clara, CA). Water was used as the mobile phase (1.0 mL/min, column temperature 35°C) for the separation of products. Agilent's pre-weighed calibration kit of Polyethylene Glycol (PEG)/Polyethylene Oxide (PEO) (part no. PL2070-020) was used to calibrate the molecular weight distribution.

Molecular dynamics simulations

The polymeric structure of PLA used to study the molecular dynamics (MD) simulations was composed of 20 monomeric units (Figure S3) with a molecular weight of ~1.5 kDa. The molecular geometries of PLA, ILs ([Ch][Lys], $[Ch]_3[Phos]$, $[C_2C_1im][Ac]$, and $[C_2C_1im]Cl$), and water were optimized using *Gaussian09* at the B3LYP level of theory and 6-311++G(d,p) basis set.[65–67] To study the microscopic interactions between PLA and IL/water mixtures, MD simulations were

carried out using the NAMD package.[68] CHARMM force field parameters were applied for all compounds under investigation. The force field parameters for ILs ([Ch][Lys], [C_2C_1im][Ac], and [C_2C_1im]Cl) and water (TIP3P water model) were based on literature[41,69,70], and for PLA and phosphate ion, the force field parameters were developed by following CHARMM-GUI tool.[71,72]

The initial configuration for all the investigated systems was prepared according to the percentage of IL to water using PACKMOL.[73] The plastic (PLA) molecule was solvated in five different solvent systems: [Ch][Lys]+water, $[Ch]_3$[Phos]+water, [C_2C_1im][Ac]+water, [C_2C_1im]Cl+water, and water. The simulation details such as the number of solvent molecules, polyester molecules, and final box size are summarized in Table S2. The potential energy of the system was first minimized for 300,000 steps using a steepest-descent algorithm. The system was then heated and equilibrated for 16 ns under the NPT ensemble using the Langevin thermostat and Nose-Hoover Langevin barostat.[74,75] SHAKE algorithm was implemented to constrain all the hydrogen involved bonds.[76] The Particle Mesh Ewald (PME) method was implemented to treat long-range electrostatic interactions at a cut-off distance of 12 Å with an accuracy of 10-6.[77] Three separate production runs with a time length of 300 ns were performed on each simulated system, starting with a different initial velocity distribution. At every 10 ps, the production coordinates were saved for structural and dynamics analysis. A 2 femtoseconds (fs) time step was used to integrate the equations of motion. All MD simulation trajectories were visualized and analyzed using TCL scripts and Visual Molecular Dynamics (VMD) tool.[78] The non-bonded interaction energies and the number of hydrogen bonds between PLA and IL/water were calculated per mole of PLA molecule.

Biological conversion

A seed culture of *P. putida* TDM461 and *P. putida* KT2440 was grown in LB broth at 30 ℃ overnight. The cell culture was centrifuged (5000 g) and washed with 3-(N-morpholino)propane sulfonic acid (MOPS) buffer five times to remove the carbon sources. 1 % cell resuspension was inoculated into 500 µL growth media in 48 well plates. The supernatant of depolymerized PET, PLA, and PET/PLA mixture (with pH adjusted to 7), synthetic TPA and LA, and glucose, were used as carbon sources with the addition of MOPS rich buffer (Teknova, #M2105) and 25 µg/mL Chloramphenicol (Table S4) in the growth media. Cell growth was monitored continuously at 600 nm (OD_{600}) for 72 h in the plate reader (Biotek-Synergy H1, Agilent, Santa Clara, CA) at 30 ℃, 570 rpm.

Techno-economic Analysis and Life-cycle Assessment

Cost and GHG emissions impacts of the one-pot PET/PLA-to-PHA conversion technology were assessed by modeling a commercial scale plastics upcycling facility in a commercial process simulation software package (SuperPro Designer V12). The capital and operating costs calculated using the process model were used to determine the minimum selling price of PHA. We assume a plant lifetime of 30 years, plant operating hours of 7920 hours (330 days/year and 24 hours/day), and an income tax of 21%.[79,80] Using the discounted cash flow rate of return (DCFROR) analysis, we determine the minimum selling price of PHA required to achieve a zero net present value with an internal rate of return (IRR) of 10%.[79]

We constructed a comprehensive life-cycle inventory for PHA production, gathering material and energy inputs and outputs for each stage of the process through rigorous material and energy balance analyses using SuperPro Designer. To determine direct and indirect GHG emissions, we used a physical units-based input-output matrix and GHG impact vectors from widely used life-

cycle assessment databases, including GREET® (Greenhouse gases, Regulated Emissions, and Energy use in Technologies) model,[81] U.S. Life Cycle Inventory Database,[82] and ecoinvent Database.[83] Our approach for life-cycle assessment is discussed in more detail in a prior study.[84]

The designed facility utilizes 100 bone-dry metric tons of plastic waste (a mixture of PET and PLA) per day and biologically converts those into PHA using an engineered *P. putida*. The overall PHA production process (Figure 6) includes plastic wastes collection and sorting, preprocessing (shredding), one-pot depolymerization and bioconversion, PHA extraction and solvent recovery, wastewater treatment, onsite energy generation (process steam), and utilities (cooling water, chilled water, and clean-in-place system).

The modeled PET and PLA upcycling facility is assumed to be co-located with a sorting facility, thus eliminating any costs and GHG emissions associated with transporting sorted and baled material from the sorting facility to the conversion facility. Prior studies have reported a wide range of material recycling cost of $69-188/metric ton, where the sorting process accounts for 30-50% of the total material recycling cost.[85–88] A few other studies have reported the sorting cost in the range of $21-32/metric ton.[89,90] Based on these prior studies, we assumed a conservative PET and PLA collection and sorting cost at the material recycling facility of $50/metric ton, nearly an average of the estimated values, for the baseline scenario. Note that this cost is largely dependent on the types of sorting technology and the waste collection mechanism.[86,89] Life-cycle GHG emissions associated with PET and PLA collection and sorting process is assumed to be 6 $kgCO_{2e}$ per metric ton of plastics.[89]

The sorted PET/PLA mixture is first sent to the preprocessing unit, where materials are shredded and stored for a short-term. Energy consumption for shredders is consistent with prior similar

studies.[80,91,92] The shredded materials are first mixed with water and cholinium lysinate ([Ch][Lys]), and then sent to the one-pot depolymerization and bioconversion reactor. We considered a batch reactor, where a series of subsequent operations are performed without removing materials, including depolymerization, cooling, pH adjustment using sulfuric acid, nutrient (nitrogen sources) loadings, inoculum and aerobic bioconversion. Operating conditions and conversion rates for PET and PLA depolymerization are based on the bench-scale experiments conducted in this study. Data inputs for the bioconversion were gathered from prior studies.[33,57–60] For the bioconversion, pressurized air is sent to a sparger at the base of the column. Air is supplied sufficient for the cell redox balancing. Table 1 summarizes the major process modeling data inputs that are considered in the current study. Additional data inputs can be found in Table S5.

Following the one pot process, a decanter centrifuge is used to separate solid and liquid. The solid fraction is sent to the PHA extraction unit and the liquid fraction is routed to the IL recovery unit. The IL is recovered using the pervaporation system, which is fully discussed in a prior study.[93] PHA is extracted using dimethyl carbonate, which is biodegradable and less harmful to humans and the environment.[94] Dimethyl carbonate is mixed with microbes-rich slurry and blended at 90°C for 1 h.[94] Residual cell mass is removed using a vacuum belt filter, and PHA is recovered from the liquid fraction by evaporating dimethyl carbonate. Dimethyl carbonate is recycled and reused. The extracted PHA is air-dried and stored onsite. The residual biomass is routed to the onsite energy generation unit. Major modeling inputs for the PHA extraction and IL recovery processes are described in Table 1.

The liquid fraction after the IL recovery is sent to the wastewater treatment unit. The wastewater includes a minimal amount of process chemicals and about 98% of water. The wastewater is first treated with NaOH and $CaCO_3$ to neutralize the remaining sulfuric and lactic acids, respectively.

Water is evaporated and reused as process water. The remaining solids are considered as a solid waste and sent to the landfill. Assumptions for the onsite energy generation and utilities are consistent with prior studies.[79,80] However, the facility only generates the required process steam; the required process electricity is sourced from the grid. Generating onsite electricity for a small-scale plastic upcycling facility considered in this study could be costly and carbon intensive, because it requires more natural gas, for example, to produce high-temperature steam for both electricity generation and process steam supply. Natural gas is used as a supplemental energy source, while the remaining solid residues after bioconversion and PHA extraction provide a small-fraction of energy to the boiler. Table S5 summarizes modeling inputs for wastewater treatment, onsite energy, and utility stages.

Acknowledgements

The authors would like to acknowledge the funding support from X the Moonshot Factory. ABPDU would also like to thank the support from The Bioenergy Technologies Office (BETO) within the US DOE's Office of Energy Efficiency and Renewable Energy. Part of this work conducted by the Joint BioEnergy Institute was supported by the Office of Science, Office of Biological and Environmental Research, of the U.S. Department of Energy under Contract No. DE-AC02-05CH11231. Sandia National Laboratories is a multi-mission laboratory managed and operated by National Technology and Engineering Solutions of Sandia, LLC, a wholly owned subsidiary of Honeywell International Inc., for the U.S. Department of Energy's National Nuclear Security Administration under contract DE-NA0003525. We would like to thank Adam Guss at the Oak Ridge National Laboratory for providing the *Pseudomonas putida* TDM461. We would also like to thank Bianca Susara who helped on the graphic abstract.

The views and opinions of the authors expressed herein do not necessarily state or reflect those of the United States Government or any agency thereof. Neither the United States Government nor any agency thereof, nor any of their employees, makes any warranty, expressed or implied, or assumes any legal liability or responsibility for the accuracy, completeness, or usefulness of any information, apparatus, product, or process disclosed or represents that its use would not infringe privately owned rights.

Author contributions

CD, HC, BAS, and NS: conceptualization and design of the work. CD, HC, ZW, MM, NRB, RAA, and SH: implementation of the work and prepare and edit the manuscript. AH, DRB, SS, CDS,

JDK, BAS, NS: review and editing the overall manuscript. Funding acquisition: led by NS, JDK, and BAS, with contributions by DRB.

Declaration of interests

The authors declare the following competing financial interest(s): CD, HC, BAS, and NS are named inventors on at least one related patent or patent application. JDK has a financial interest in Amyris, Lygos, Demetrix, Napigen, Maple Bio, Apertor Labs, Berkeley Yeast, Ansa Biotechnologies, Cyklos Materials, and Zero Acre Farms. CDS has a financial interest in Cyklos Materials. The authors have no other relevant affiliations or financial involvement with any organization or entity with a financial interest in or financial conflict with the subject matter or materials discussed in the manuscript apart from those disclosed. No writing assistance was utilized in the production of this manuscript.

Inclusion and Diversity

We support inclusive, diverse, and equitable conduct of research.

Figures

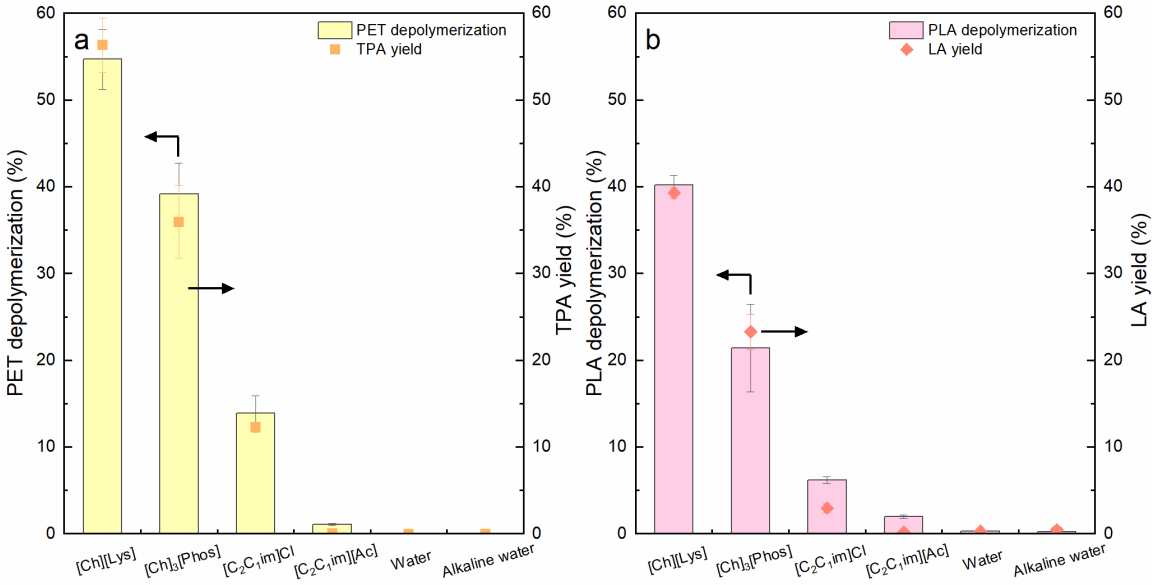

Figure 1. Depolymerization efficiency and product yield of individual polyesters.

(A) PET at 180 °C and (B) PLA at 130 °C with polymer solid loading at 10 wt% in the presence or absence of 10 wt% ILs for 2 h. Data are represented as mean ± Standard Deviation (SD).

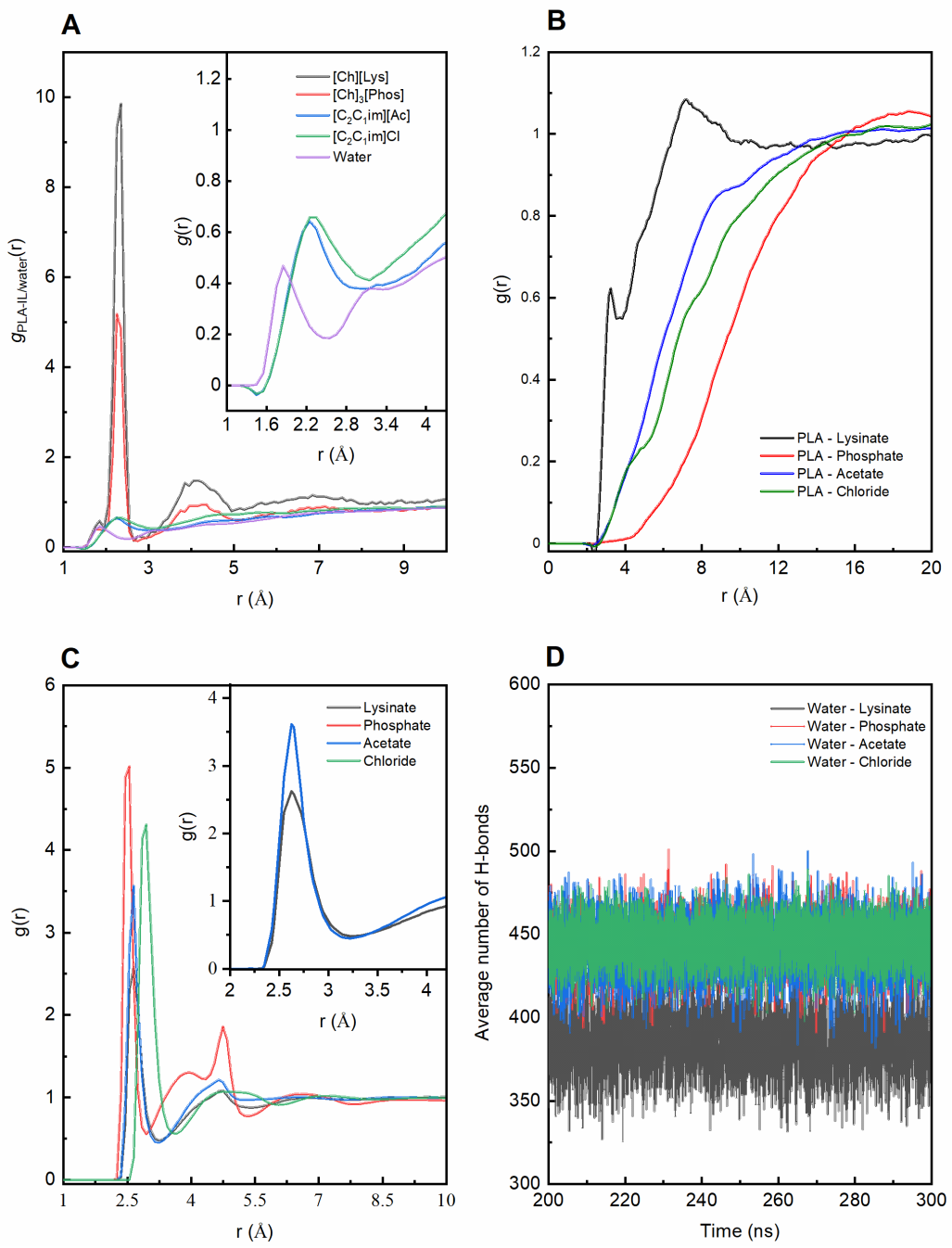

Figure 2. Radial distribution function (RDF) and average number of hydrogen bonds in different PLA/IL/water systems.

(A) RDF between the oxygen (O) atom of PLA with cation or water. (B) RDF between the oxygen (O) atom of PLA with anions. (C) RDF between IL anion and water. (D) average number of hydrogen bonds between IL anion and water.

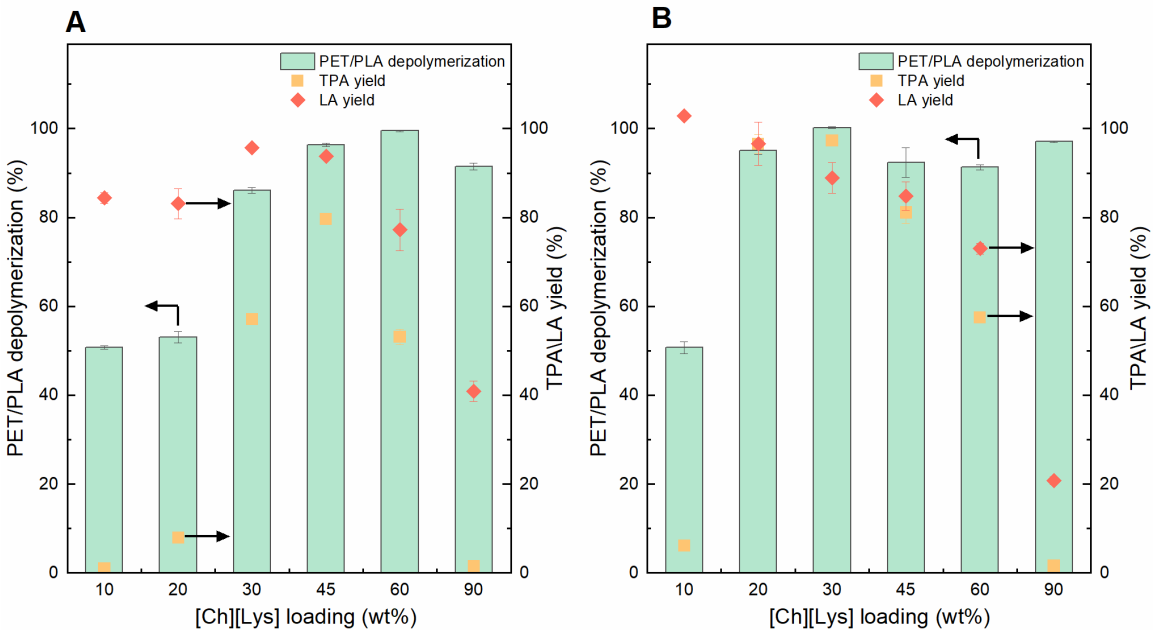

Figure 3. Depolymerization efficiency and product yields of PET/PLA mixture.

(A) 2h and (B) 6h reactions with polymer solid loading at 10 wt% using different [Ch][Lys] loadings at 160 °C. Data are represented as mean ± SD.

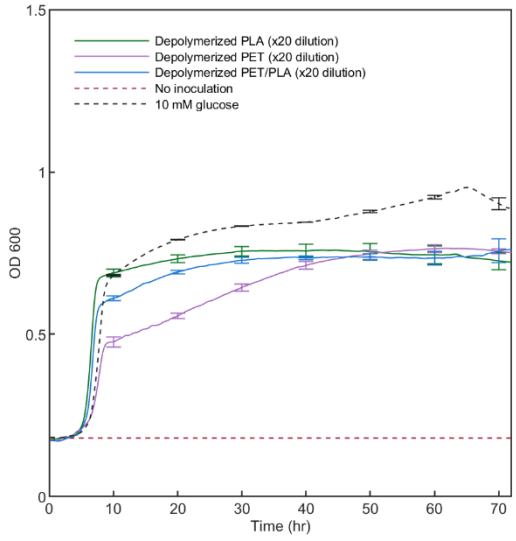

Figure 4. Impact of carbon source on *P. putida* TDM461 cell growth.

Plots of cell growth in depolymerized PET, PLA, and PET/PLA mixture in comparison with controls (10 mM glucose and no inoculation). Three biological replicates were performed. Data are represented as mean ± SD. See Figure S7 for detailed growth curves.

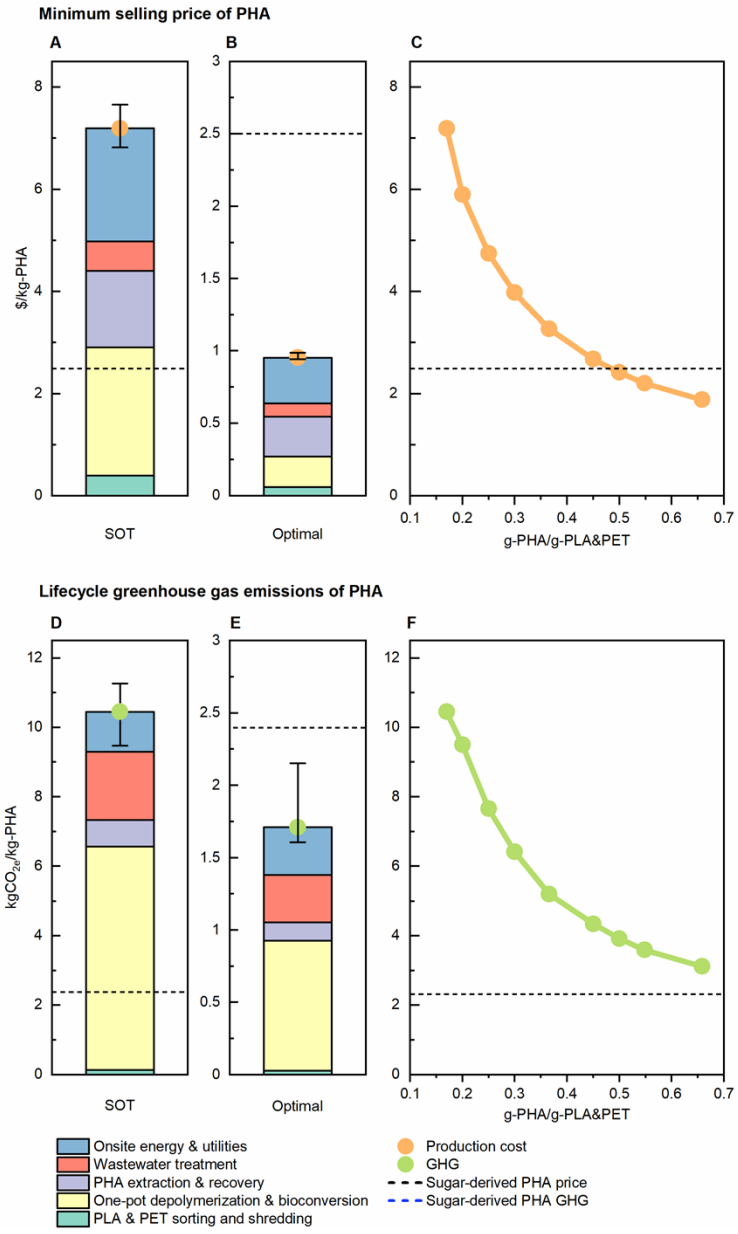

Figure 5. Production cost and carbon footprint of biologically produced PHA.

(A, D) the current state of technology, (B, E) the optimal future case, (C, F) the production cost and GHG emissions of PHA as a function of yield, with other input parameters remaining the same as baseline values (Table 1 and Table S5). SOT = current state of the technology and Optimal = future scenario with improved conversion efficiency (Table 1 and Table S5). The horizontal dashed lines represent the selling price ($2.5/kg)[62] and carbon footprint (2.4 $kgCO_{2e}$/kg) of sugar-derived PHA.[61] A PHA yield of 49.7 g per 100 g of PET/PLA mixture is required to reach cost-parity with sugar-derived PHA (Figure C).

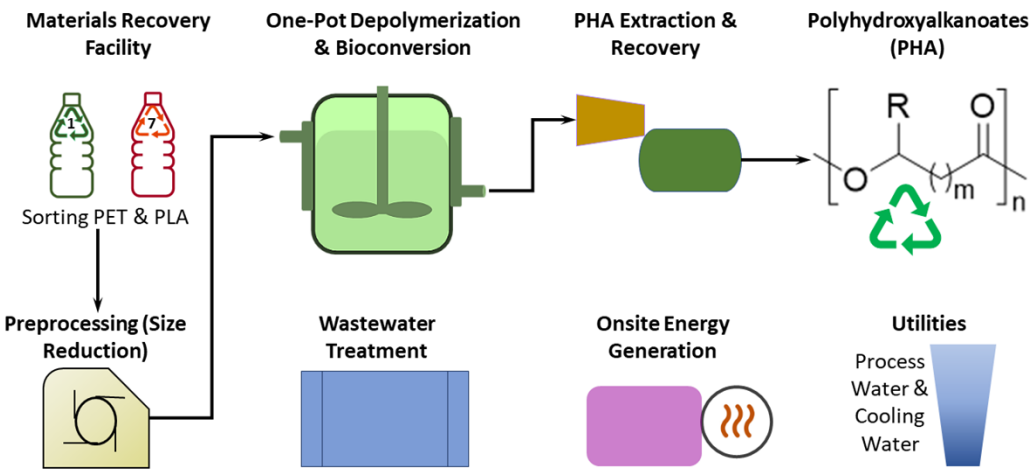

Figure 6. System boundary for techno-economic assessment and life-cycle analysis.

Overview of one-pot conversion process of PET/PLA mixture into polyhydroxyalkanoates (PHA).

Tables

Table 1. Major process modeling inputs used to develop PLA and PET upcycling model in this study

Parameters	Units	State of technology	Optimal future case
Scale of the plastic upcycling facility[86]	bone-dry metric ton (bdt)/day	100	200
PET/PLA collection and sorting cost[86,89,90,95]	$/bdt	50	32
PET/PLA collection and sorting emissions[89]	$kgCO_{2e}$/bdt	6	6
PET/PLA composition			
PET	wt%	50	50
PLA	wt%	50	50
One-pot depolymerization and bioconversion			
Solid loading	wt%	10[a]	30
Ionic liquid (IL) loading	wt%	20[a]	15
Depolymerization time	h	6[a]	6
PET/PLA depolymerization rate	%	95[a]	99
Bioconversion time[57]	h	27	24
TPA to PHA[b]	% of theoretical yield	9.5[33]	90
LA to PHA[b]	% of theoretical yield	37.6[59,60]	90
EG to PHA[b]	% of theoretical yield	9.6[58]	90
Recovery and separation			
PHA recovery[94]	%	95	98
IL recovery[93]	%	97	99

[a]Based on the experimental data demonstrated in this study.

[b]Stoichiometric theoretical yields of PHA from TPA, LA, and EG are estimated to be 79.3, 58.5, 62.3 g per 100 g of substrate, respectively. The detailed method is illustrated in a prior study.[96] Please note that the biological yields would be lower than these stoichiometric yields. We assumed 90% of the stoichiometric theoretical yield for the optimal future case, assuming that future research will improve bioconversion efficiency similar to ethanol produced in *Z. mobilis*.[80]

References

Bibliography

1. PlasticsEurope, and EPRO (2022). Plastics—the facts 2022. An analysis of European plastics production, demand and waste data (PlasticsEurope).
2. Napper, I.E., Davies, B.F.R., Clifford, H., Elvin, S., Koldewey, H.J., Mayewski, P.A., Miner, K.R., Potocki, M., Elmore, A.C., Gajurel, A.P., et al. (2020). Reaching new heights in plastic pollution—preliminary findings of microplastics on mount everest. One Earth *3*, 621–630.
3. Willis, K., Hardesty, B.D., Vince, J., and Wilcox, C. (2022). Local waste management successfully reduces coastal plastic pollution. One Earth *5*, 666–676.
4. Bauer, F., Nielsen, T.D., Nilsson, L.J., Palm, E., Ericsson, K., Fråne, A., and Cullen, J. (2022). Plastics and climate change—Breaking carbon lock-ins through three mitigation pathways. One Earth *5*, 361–376.
5. World Economic Forum, Ellen MacArthur Foundation, and Co., M.& (2016). The New Plastics Economy: Rethinking the future of plastics. https://www.weforum.org/reports/the-new-plastics-economy-rethinking-the-future-of-plastics.
6. Closing the plastics loop (2018). Nat. Sustain. *1*, 205–205.
7. Tullo, A. (2018). Should plastics be a source of energy? C&EN Global Enterp. *96*, 34–39.
8. Carné Sánchez, A., and Collinson, S.R. (2011). The selective recycling of mixed plastic waste of polylactic acid and polyethylene terephthalate by control of process conditions. Eur. Polym. J. *47*, 1970–1976.
9. Waste Management World (2009). NAPCOR concerned over PLA contamination of PET stream. https://waste-management-world.com/a/napcor-concerned-over-pla-contamination-of-pet-stream.
10. Alaerts, L., Augustinus, M., and Van Acker, K. (2018). Impact of Bio-Based Plastics on Current Recycling of Plastics. Sustainability *10*, 1487.
11. Taneepanichskul, N., Purkiss, D., and Miodownik, M. (2022). A review of sorting and separating technologies suitable for compostable and biodegradable plastic packaging. Front. Sustain. *3*.
12. Barnard, E., Rubio Arias, J.J., and Thielemans, W. (2021). Chemolytic depolymerisation of PET: a review. Green Chem. *23*, 3765–3789.
13. Rahimi, A., and García, J.M. (2017). Chemical recycling of waste plastics for new materials production. Nat. rev. chem. *1*, 0046.
14. Conk, R.J., Hanna, S., Shi, J.X., Yang, J., Ciccia, N.R., Qi, L., Bloomer, B.J., Heuvel, S., Wills, T., Su, J., et al. (2022). Catalytic deconstruction of waste polyethylene with ethylene to form propylene. Science *377*, 1561–1566.
15. Bunescu, A., Lee, S., Li, Q., and Hartwig, J.F. (2017). Catalytic hydroxylation of polyethylenes. ACS Cent. Sci. *3*, 895–903.
16. Celik, G., Kennedy, R.M., Hackler, R.A., Ferrandon, M., Tennakoon, A., Patnaik, S., LaPointe, A.M., Ammal, S.C., Heyden, A., Perras, F.A., et al. (2019). Upcycling Single-Use Polyethylene into

High-Quality Liquid Products. ACS Cent. Sci. *5*, 1795–1803.

17. Zichittella, G., Ebrahim, A.M., Zhu, J., Brenner, A.E., Drake, G., Beckham, G.T., Bare, S.R., Rorrer, J.E., and Román-Leshkov, Y. (2022). Hydrogenolysis of Polyethylene and Polypropylene into Propane over Cobalt-Based Catalysts. JACS Au *2*, 2259–2268.
18. Jehanno, C., Pérez-Madrigal, M.M., Demarteau, J., Sardon, H., and Dove, A.P. (2019). Organocatalysis for depolymerisation. Polym. Chem. *10*, 172–186.
19. Sullivan, K.P., Werner, A.Z., Ramirez, K.J., Ellis, L.D., Bussard, J.R., Black, B.A., Brandner, D.G., Bratti, F., Buss, B.L., Dong, X., et al. (2022). Mixed plastics waste valorization through tandem chemical oxidation and biological funneling. Science *378*, 207–211.
20. Sui, X., Zhang, L., Li, J., Doyle-Davis, K., Li, R., Wang, Z., and Sun, X. (2022). Advanced support materials and interactions for atomically dispersed noble-metal catalysts: from support effects to design strategies. Adv. Energy Mater. *12*.
21. Bai, P., Etim, U.J., Yan, Z., Mintova, S., Zhang, Z., Zhong, Z., and Gao, X. (2018). Fluid catalytic cracking technology: current status and recent discoveries on catalyst contamination. Catalysis Reviews, 1–73.
22. Lei, Z., Chen, B., Koo, Y.-M., and MacFarlane, D.R. (2017). Introduction: Ionic Liquids. Chem. Rev. *117*, 6633–6635.
23. Amarasekara, A.S. (2016). Acidic Ionic Liquids. Chem. Rev. *116*, 6133–6183.
24. Xin, J., Zhang, Q., Huang, J., Huang, R., Jaffery, Q.Z., Yan, D., Zhou, Q., Xu, J., and Lu, X. (2021). Progress in the catalytic glycolysis of polyethylene terephthalate. J. Environ. Manage. *296*, 113267.
25. Feghali, E., Tauk, L., Ortiz, P., Vanbroekhoven, K., and Eevers, W. (2020). Catalytic chemical recycling of biodegradable polyesters. Polym. Degrad. Stab. *179*, 109241.
26. Liu, M., Guo, J., Gu, Y., Gao, J., and Liu, F. (2018). Versatile Imidazole-Anion-Derived Ionic Liquids with Unparalleled Activity for Alcoholysis of Polyester Wastes under Mild and Green Conditions. ACS Sustain. Chem. Eng. *6*, 15127–15134.
27. Liu, F., Cui, X., Yu, S., Li, Z., and Ge, X. (2009). Hydrolysis reaction of poly(ethylene terephthalate) using ionic liquids as solvent and catalyst. J. Appl. Polym. Sci. *114*, 3561–3565.
28. Song, X., Wang, H., Yang, X., Liu, F., Yu, S., and Liu, S. (2014). Hydrolysis of poly(lactic acid) into calcium lactate using ionic liquid [Bmim][OAc] for chemical recycling. Polym. Degrad. Stab. *110*, 65–70.
29. Hara, H., Eltis, L.D., Davies, J.E., and Mohn, W.W. (2007). Transcriptomic analysis reveals a bifurcated terephthalate degradation pathway in Rhodococcus sp. strain RHA1. J. Bacteriol. *189*, 1641–1647.
30. Narancic, T., Salvador, M., Hughes, G.M., Beagan, N., Abdulmutalib, U., Kenny, S.T., Wu, H., Saccomanno, M., Um, J., O'Connor, K.E., et al. (2021). Genome analysis of the metabolically versatile Pseudomonas umsongensis GO16: the genetic basis for PET monomer upcycling into polyhydroxyalkanoates. Microb. Biotechnol. *14*, 2463–2480.
31. Sasoh, M., Masai, E., Ishibashi, S., Hara, H., Kamimura, N., Miyauchi, K., and Fukuda, M. (2006). Characterization of the terephthalate degradation genes of Comamonas sp. strain E6. Appl. Environ.

Microbiol. *72*, 1825–1832.

32. Yoshida, S., Hiraga, K., Takehana, T., Taniguchi, I., Yamaji, H., Maeda, Y., Toyohara, K., Miyamoto, K., Kimura, Y., and Oda, K. (2016). A bacterium that degrades and assimilates poly(ethylene terephthalate). Science *351*, 1196–1199.

33. Kenny, S.T., Runic, J.N., Kaminsky, W., Woods, T., Babu, R.P., Keely, C.M., Blau, W., and O'Connor, K.E. (2008). Up-cycling of PET (polyethylene terephthalate) to the biodegradable plastic PHA (polyhydroxyalkanoate). Environ. Sci. Technol. *42*, 7696–7701.

34. Tran, T.T., and Charles, T.C. (2020). Lactic acid containing polymers produced in engineered Sinorhizobium meliloti and Pseudomonas putida. PLoS ONE *15*, e0218302.

35. Liu, Y., Yao, X., Yao, H., Zhou, Q., Xin, J., Lu, X., and Zhang, S. (2020). Degradation of poly(ethylene terephthalate) catalyzed by metal-free choline-based ionic liquids. Green Chem. *22*, 3122–3131.

36. Sun, J., Liu, D., Young, R.P., Cruz, A.G., Isern, N.G., Schuerg, T., Cort, J.R., Simmons, B.A., and Singh, S. (2018). Solubilization and Upgrading of High Polyethylene Terephthalate Loadings in a Low-Costing Bifunctional Ionic Liquid. ChemSusChem *11*, 781–792.

37. Allen, J.J., Bowser, S.R., and Damodaran, K. (2014). Molecular interactions in the ionic liquid emim acetate and water binary mixtures probed via NMR spin relaxation and exchange spectroscopy. Phys. Chem. Chem. Phys. *16*, 8078–8085.

38. Yagihashi, M., and Funazukuri, T. (2010). Recovery ofl -Lactic Acid from Poly(l -lactic acid) under Hydrothermal Conditions of Dilute Aqueous Sodium Hydroxide Solution. Ind. Eng. Chem. Res. *49*, 1247–1251.

39. Karayannidis, G.P., Chatziavgoustis, A.P., and Achilias, D.S. (2002). Poly(ethylene terephthalate) recycling and recovery of pure terephthalic acid by alkaline hydrolysis. Adv. Polym. Technol. *21*, 250–259.

40. Mishra, S., and Goje, A.S. (2003). Chemical recycling, kinetics, and thermodynamics of alkaline depolymerization of waste poly (ethylene terephthalate) (PET). Polymer Reaction Engineering *11*, 963–987.

41. Mohan, M., Choudhary, H., George, A., Simmons, B.A., Sale, K., and Gladden, J.M. (2021). Towards understanding of delignification of grassy and woody biomass in cholinium-based ionic liquids. Green Chem. *23*, 6020–6035.

42. Hou, X.-D., Liu, Q.-P., Smith, T.J., Li, N., and Zong, M.-H. (2013). Evaluation of toxicity and biodegradability of cholinium amino acids ionic liquids. PLoS ONE *8*, e59145.

43. Xu, F., Sun, J., Konda, N.V.S.N.M., Shi, J., Dutta, T., Scown, C.D., Simmons, B.A., and Singh, S. (2016). Transforming biomass conversion with ionic liquids: process intensification and the development of a high-gravity, one-pot process for the production of cellulosic ethanol. Energy Environ. Sci. *9*, 1042–1049.

44. Wang, H., Li, Z., Liu, Y., Zhang, X., and Zhang, S. (2009). Degradation of poly(ethylene terephthalate) using ionic liquids. Green Chem. *11*, 1568.

45. Li, X.-Y., Zhou, Q., Yang, K.-K., and Wang, Y.-Z. (2014). Degradation of polylactide using basic

ionic liquid imidazolium acetates. Chem. Pap. *68*, 1375–1380.

46. Barcelos, C.A., Oka, A.M., Yan, J., Das, L., Achinivu, E.C., Magurudeniya, H., Dong, J., Akdemir, S., Baral, N.R., Yan, C., et al. (2021). High-Efficiency Conversion of Ionic Liquid-Pretreated Woody Biomass to Ethanol at the Pilot Scale. ACS Sustain. Chem. Eng. *9*, 4042–4053.

47. Magurudeniya, H.D., Baral, N.R., Rodriguez, A., Scown, C.D., Dahlberg, J., Putnam, D., George, A., Simmons, B.A., and Gladden, J.M. (2021). Use of ensiled biomass sorghum increases ionic liquid pretreatment efficiency and reduces biofuel production cost and carbon footprint. Green Chem. *23*, 3127–3140.

48. Kenny, S.T., Runic, J.N., Kaminsky, W., Woods, T., Babu, R.P., and O'Connor, K.E. (2012). Development of a bioprocess to convert PET derived terephthalic acid and biodiesel derived glycerol to medium chain length polyhydroxyalkanoate. Appl. Microbiol. Biotechnol. *95*, 623–633.

49. Lim, H.G., Fong, B., Alarcon, G., Magurudeniya, H.D., Eng, T., Szubin, R., Olson, C.A., Palsson, B.O., Gladden, J.M., Simmons, B.A., et al. (2020). Generation of ionic liquid tolerant *Pseudomonas putida* KT2440 strains *via* adaptive laboratory evolution. Green Chem. *22*, 5677–5690.

50. Mohamed, E.T., Werner, A.Z., Salvachúa, D., Singer, C.A., Szostkiewicz, K., Rafael Jiménez-Díaz, M., Eng, T., Radi, M.S., Simmons, B.A., Mukhopadhyay, A., et al. (2020). Adaptive laboratory evolution of Pseudomonas putida KT2440 improves p-coumaric and ferulic acid catabolism and tolerance. Metab. Eng. Commun. *11*, e00143.

51. Werner, A.Z., Clare, R., Mand, T.D., Pardo, I., Ramirez, K.J., Haugen, S.J., Bratti, F., Dexter, G.N., Elmore, J.R., Huenemann, J.D., et al. (2021). Tandem chemical deconstruction and biological upcycling of poly(ethylene terephthalate) to β-ketoadipic acid by Pseudomonas putida KT2440. Metab. Eng. *67*, 250–261.

52. Yao, A., Choudhary, H., Mohan, M., Rodriguez, A., Magurudeniya, H., Pelton, J.G., George, A., Simmons, B.A., and Gladden, J.M. (2021). Can multiple ions in an ionic liquid improve the biomass pretreatment efficacy? ACS Sustain. Chem. Eng. *12*, 4371–4376.

53. Park, M., Chen, Y., Thompson, M., Benites, V.T., Fong, B., Petzold, C.J., Baidoo, E.E.K., Gladden, J.M., Adams, P.D., Keasling, J.D., et al. (2020). Response of *Pseudomonas putida* to Complex, Aromatic-Rich Fractions from Biomass. ChemSusChem *13*, 1–14.

54. Belda, E., van Heck, R.G.A., José Lopez-Sanchez, M., Cruveiller, S., Barbe, V., Fraser, C., Klenk, H.-P., Petersen, J., Morgat, A., Nikel, P.I., et al. (2016). The revisited genome of Pseudomonas putida KT2440 enlightens its value as a robust metabolic chassis. Environ. Microbiol. *18*, 3403–3424.

55. Wargo, M.J., Szwergold, B.S., and Hogan, D.A. (2008). Identification of two gene clusters and a transcriptional regulator required for Pseudomonas aeruginosa glycine betaine catabolism. J. Bacteriol. *190*, 2690–2699.

56. Weimer, A., Kohlstedt, M., Volke, D.C., Nikel, P.I., and Wittmann, C. (2020). Industrial biotechnology of Pseudomonas putida: advances and prospects. Appl. Microbiol. Biotechnol. *104*, 7745–7766.

57. Tiso, T., Narancic, T., Wei, R., Pollet, E., Beagan, N., Schröder, K., Honak, A., Jiang, M., Kenny, S.T., Wierckx, N., et al. (2021). Towards bio-upcycling of polyethylene terephthalate. Metab. Eng.

66, 167–178.

58. Franden, M.A., Jayakody, L.N., Li, W.-J., Wagner, N.J., Cleveland, N.S., Michener, W.E., Hauer, B., Blank, L.M., Wierckx, N., Klebensberger, J., et al. (2018). Engineering Pseudomonas putida KT2440 for efficient ethylene glycol utilization. Metab. Eng. *48*, 197–207.

59. Shi, H., Shiraishi, M., and Shimizu, K. (1997). Metabolic flux analysis for biosynthesis of poly(β-hydroxybutyric acid) in Alcaligenes eutrophus from various carbon sources. Journal of Fermentation and Bioengineering *84*, 579–587.

60. Tanaka, K., Katamune, K., and Ishizaki, A. (1995). Fermentative production of poly(β-hydroxybutyric acid) from xylose viaL -lactate by a two-stage culture method employing *Lactococcus lactis* IO-1 and *Alcaligenes eutrophus*. Can. J. Microbiol. *41*, 257–261.

61. Gerngross, T.U. (1999). Can biotechnology move us toward a sustainable society? Nat. Biotechnol. *17*, 541–544.

62. Slome, S. (2019). Biorenewable Insights: Bio-Polymers for Food Applications (NexantECA).

63. Vora, N., Christensen, P.R., Demarteau, J., Baral, N.R., Keasling, J.D., Helms, B.A., and Scown, C.D. (2021). Leveling the cost and carbon footprint of circular polymers that are chemically recycled to monomer. Sci. Adv. *7*, eabf0187.

64. Statista (2022). Polyethylene terephthalate prices globally. https://www.statista.com/statistics/1171088/price-polyethylene-terephthalate-forecast-globally/.

65. Zhang, Y., He, H., Dong, K., Fan, M., and Zhang, S. (2017). A DFT study on lignin dissolution in imidazolium-based ionic liquids. RSC Adv. *7*, 12670–12681.

66. Mohan, M., Banerjee, T., and Goud, V.V. (2018). COSMO-RS-Based Screening of Antisolvents for the Separation of Sugars from Ionic Liquids: Experimental and Molecular Dynamic Simulations. ACS Omega *3*, 7358–7370.

67. Schlegel, H.B., Scuseria, G.E., Robb, M.A., and Cheeseman, J.R. (2009). Gaussian 09 (Gaussian, Inc.).

68. Phillips, J.C., Braun, R., Wang, W., Gumbart, J., Tajkhorshid, E., Villa, E., Chipot, C., Skeel, R.D., Kalé, L., and Schulten, K. (2005). Scalable molecular dynamics with NAMD. J. Comput. Chem. *26*, 1781–1802.

69. Mohan, M., Viswanath, P., Banerjee, T., and Goud, V.V. (2018). Multiscale modelling strategies and experimental insights for the solvation of cellulose and hemicellulose in ionic liquids. Mol. Phys. *116*, 1–21.

70. Mohan, M., Banerjee, T., and Goud, V.V. (2016). Effect of protic and aprotic solvents on the mechanism of cellulose dissolution in ionic liquids: A combined molecular dynamics and experimental insight. ChemistrySelect *1*, 4823–4832.

71. Jo, S., Kim, T., Iyer, V.G., and Im, W. (2008). CHARMM-GUI: a web-based graphical user interface for CHARMM. J. Comput. Chem. *29*, 1859–1865.

72. Kim, S., Lee, J., Jo, S., Brooks, C.L., Lee, H.S., and Im, W. (2017). CHARMM-GUI ligand reader and modeler for CHARMM force field generation of small molecules. J. Comput. Chem. *38*, 1879–1886.

73. Martínez, L., Andrade, R., Birgin, E.G., and Martínez, J.M. (2009). PACKMOL: a package for building initial configurations for molecular dynamics simulations. J. Comput. Chem. *30*, 2157–2164.

74. Martyna, G.J., Tobias, D.J., and Klein, M.L. (1994). Constant pressure molecular dynamics algorithms. J. Chem. Phys. *101*, 4177.

75. Feller, S.E., Zhang, Y., Pastor, R.W., and Brooks, B.R. (1995). Constant pressure molecular dynamics simulation: The Langevin piston method. J. Chem. Phys. *103*, 4613–4621.

76. Allen, M.P., and Tildesley, D.J. (2017). Computer simulation of liquids 2nd ed. (Oxford University Press).

77. Leeuw, S.W. de, Perram, J.W., and Smith, E.R. (1983). Simulation of electrostatic systems in periodic boundary conditions. III. Further theory and applications. Proc. R. Soc. Lond. A *388*, 177–193.

78. Humphrey, W., Dalke, A., and Schulten, K. (1996). VMD: visual molecular dynamics. J. Mol. Graph. *14*, 33–8, 27.

79. Davis, R.E., Grundl, N.J., Tao, L., Biddy, M.J., Tan, E.C., Beckham, G.T., Humbird, D., Thompson, D.N., and Roni, M.S. (2018). Process design and economics for the conversion of lignocellulosic biomass to hydrocarbon fuels and coproducts: 2018 biochemical design case update; biochemical deconstruction and conversion of biomass to fuels and products via integrated biorefinery pathways (National Renewable Energy Laboratory (NREL)).

80. Humbird, D., Davis, R., Tao, L., Kinchin, C., Hsu, D., Aden, A., Schoen, P., Lukas, J., Olthof, B., Worley, M., et al. (2011). Process Design and Economics for Biochemical Conversion of Lignocellulosic Biomass to Ethanol: Dilute-Acid Pretreatment and Enzymatic Hydrolysis of Corn Stover (National Renewable Energy Laboratory (NREL)).

81. Argonne National Laboratory (2021). Greenhouse gases, Regulated Emissions, and Energy use in Technologies Model ® GREET. https://greet.es.anl.gov/.

82. National Renewable Energy Laboratory (NREL) (2012). U.S. Life Cycle Inventory Database. https://www.lcacommons.gov/nrel/search.

83. Ecoinvent The ecoinvent Database. https://ecoinvent.org/the-ecoinvent-database/.

84. Neupane, B., Konda, N.V.S.N.M., Singh, S., Simmons, B.A., and Scown, C.D. (2017). Life-cycle greenhouse gas and water intensity of cellulosic biofuel production using cholinium lysinate ionic liquid pretreatment. ACS Sustain. Chem. Eng. *5*, 10176–10185.

85. Improving Oregon Recycling Systems Infrastructure Research (2020). (Cascadia Consulting Group).

86. Materials Recovery Facility (MRF) Feasibility Study (2018). (Metro Waste Authority).

87. Northeast Recycling Council (NERC) (2020). Report on Blended MRF Values - EPA Regions 1, 2 and 3 (The Northeast Recycling Council (NERC)).

88. Cimpan, C., Maul, A., Wenzel, H., and Pretz, T. (2016). Techno-economic assessment of central sorting at material recovery facilities – the case of lightweight packaging waste. J. Clean. Prod. *112*, 4387–4397.

89. Volk, R., Stallkamp, C., Steins, J.J., Yogish, S.P., Müller, R.C., Stapf, D., and Schultmann, F. (2021). Techno-economic assessment and comparison of different plastic recycling pathways: A German case study. Journal of Industrial Ecology *25*, 1318–1337.

90. Chaudhari, U.S., Lin, Y., Thompson, V.S., Handler, R.M., Pearce, J.M., Caneba, G., Muhuri, P., Watkins, D., and Shonnard, D.R. (2021). Systems analysis approach to polyethylene terephthalate and olefin plastics supply chains in the circular economy: A review of data sets and models. ACS Sustain. Chem. Eng. *22*, 7403–7421.

91. Larrain, M., Van Passel, S., Thomassen, G., Van Gorp, B., Nhu, T.T., Huysveld, S., Van Geem, K.M., De Meester, S., and Billen, P. (2021). Techno-economic assessment of mechanical recycling of challenging post-consumer plastic packaging waste. Resources, Conservation and Recycling *170*, 105607.

92. Jacobson, J.J., Roni, M.S., Lamers, P., and Cafferty, K.G. (2014). Biomass feedstock and conversion supply system design and analysis (Idaho National Laboratory).

93. Sun, J., Shi, J., Murthy Konda, N.V.S.N., Campos, D., Liu, D., Nemser, S., Shamshina, J., Dutta, T., Berton, P., Gurau, G., et al. (2017). Efficient dehydration and recovery of ionic liquid after lignocellulosic processing using pervaporation. Biotechnol. Biofuels *10*, 154.

94. Samorì, C., Basaglia, M., Casella, S., Favaro, L., Galletti, P., Giorgini, L., Marchi, D., Mazzocchetti, L., Torri, C., and Tagliavini, E. (2015). Dimethyl carbonate and switchable anionic surfactants: two effective tools for the extraction of polyhydroxyalkanoates from microbial biomass. Green Chem. *17*, 1047–1056.

95. Husock, H. (2020). A Cost-Benefit Analysis of Recycling in The U.S. (Manhattan Institute).

96. Dunlop, M.J., Dossani, Z.Y., Szmidt, H.L., Chu, H.C., Lee, T.S., Keasling, J.D., Hadi, M.Z., and Mukhopadhyay, A. (2011). Engineering microbial biofuel tolerance and export using efflux pumps. Mol. Syst. Biol. *7*, 487.